Available online at www.sciencedirect.com

ScienceDirect

Ceramics International 41 (2015) 4161–4168

CERAMICS INTERNATIONAL

www.elsevier.com/locate/ceramint

Synthesis and properties of CuO-doped $Ce_{0.9}Gd_{0.1}O_{2-\delta}$ electrolytes for SOFCs

Chrystian G.M. Lima[a], Thamyscira H. Santos[a], João P.F. Grilo[b], Ricardo P.S. Dutra[a], Rubens M. Nascimento[b], Surendran Rajesh[c], Fábio C. Fonseca[d], Daniel A. Macedo[a,*]

[a]Materials Science and Engineering Postgraduate Program, UFPB, 58051-900 João Pessoa, Brazil
[b]Materials Science and Engineering Postgraduate Program, UFRN, 59078-970 Natal, Brazil
[c]Department of Materials & Ceramic Engineering/CICECO, University of Aveiro, 3810-193 Aveiro, Portugal
[d]Energy and Nuclear Research Institute, IPEN, 05508-900 São Paulo, Brazil

Received 20 September 2014; received in revised form 12 December 2014; accepted 16 December 2014
Available online 23 December 2014

Abstract

The effects of copper oxide (CuO) addition on the crystal structure, densification and microstructure of Gd-doped ceria ($Ce_{0.9}Gd_{0.1}O_{2-\delta}$, CGO) synthesized by the polymeric precursor method have been studied. $Ce_{0.9-x}Gd_{0.1}Cu_xO_{2-\delta}$ ($0 \le x \le 0.01$) precursor powders were calcined at 600 °C for 1 h and the phase formation was studied by powder X-ray diffraction combined with Rietveld refinement analysis. Relative density measurements and microstructural analysis were performed on pellets sintered in the temperature range 1000–1100 °C in air. The effect of CuO as a sintering aid becomes more visible when its content is in the 0.5–1 mol% range where the relative densities are found to be 98% for sintering temperature as low as 1000 °C. A remarkable reduction (up to ~500 °C) in the sintering temperature for 1 mol% CuO-doped CGO ceramics is observed together with the formation of a dissolved phase of Gd_2O_3–CeO_2–CuO. $Ce_{0.89}Gd_{0.1}Cu_{0.01-y}O_{2-\delta}$ sintered at 1000 °C shows total electrical conductivity of 15.5 mS cm^{-1} at 600 °C slightly higher than $Ce_{0.9}Gd_{0.1}O_{2-\delta}$ sintered at 1500 °C (12.4 mS cm^{-1}).

Keywords: Gadolinia-doped ceria; Sintering aid; Microstructure; Electrical conductivity

1. Introduction

Solid solutions of ceria doped with rare earth elements (Gd^{3+}, Sm^{3+}, Y^{3+}, Nd^{3+}, La^{3+}, etc.) are widely regarded as promising electrolyte materials for intermediate and low temperature solid oxide fuel cells (SOFCs) since their ionic conductivities are four to five times higher than that of the yttria-stabilized zirconia (YSZ), in oxidizing atmosphere [1,2]. In order to minimize the activation enthalpy of the ionic conduction process in doped ceria electrolytes, it has been pointed out that the radius of the dopant cation should be close to that of the host (R^{4+}_{ce}=0.97 Å). However, there is a controversy concerning the trivalent dopant that promotes the highest ionic conductivity, although both Gd^{3+} (R^{3+}_{Gd}=1.053 Å) and Sm^{3+} (R^{3+}_{Sm}=1.079 Å) have been reported to perform better than other trivalent lanthanides showing similar conductivity values [3–5]. Despite the improved electrical properties as compared to YSZ ceramics, one of the main drawbacks of ceria-based electrolytes is the high sintering temperatures (1350–1600 °C) required for full densification [6,7]. Such high temperature sintering has several disadvantages such as high manufacturing cost, reduction of Ce^{4+}–Ce^{3+}, and failure of co-firing with electrodes during fabrication of cathode or anode supported SOFCs.

In order to improve the sinterability of doped ceria ceramics, two processing alternatives had been widely used. The first approach is to use highly reactive powders derived from wet chemical routes, such as co-precipitation, sol–gel, spray pyrolysis, and the polymeric precursor method [8–11]. In the second approach, ceria-based ceramics have been sintered at lower temperatures by the addition

*Corresponding author. Tel.: +55 83 3216 7076; fax: +55 83 3216 7905.
E-mail address: damaced@gmail.com (D.A. Macedo).

http://dx.doi.org/10.1016/j.ceramint.2014.12.093
0272-8842/

of low melting-point sintering aids (mostly transition metal oxides such as CuO, Bi_2O_3, $CoO_{1.333}$, and MnO_2) into commercial or synthesized powders [12–15].

The present study reports on the preparation of 10 mol% Gd-doped ceria ($Ce_{0.9}Gd_{0.1}O_{2-\delta}$, CGO) with small additions of copper oxide (from 0 to 1 mol%), used as sintering aid, via the polymeric precursor method. CuO was selected based on the promising results presented by Dong et al. [12,16] for powders synthesized by the polyvinyl alcohol assisted combustion method. The effect of CuO amount on the structure of calcined powders, densification and microstructure of sintered ceramics has been evaluated. Additionally, a preliminary electrical characterization of samples with and without 1 mol% CuO addition was carried out by electrochemical impedance spectroscopy.

2. Experimental

CuO-doped $Ce_{0.9}Gd_{0.1}O_{2-\delta}$ (CuO-CGO) powders with nominal compositions $Ce_{0.9-x}Gd_{0.1}Cu_xO_{2-\delta}$ ($0 \le x \le 0.01$) were synthesized by the polymeric precursor method. The starting materials were as follows: cerium, gadolinium and copper nitrates (Sigma Aldrich, USA); citric acid (Synth, Brazil); and ethylene glycol (Synth, Brazil).

The polymeric precursor method consists of the formation of a chelate of the cations with a hydroxycarboxylic acid, more often citric acid. Later, a polyhydroxy alcohol, generally ethylene glycol, is added to it. Upon heating, the polyesterification reaction takes place and, a primary heating in an oxidizing atmosphere about 250–350 °C produces the precursor powder. The thermal treatment of the precursor at an adequate temperature yields a ceramic powder, with a higher sinterability than powders synthesized by solid state reaction. The polymeric precursor method also possesses other advantages such as excellent homogeneity, good stoichiometric control and superior control over the particle morphology [17,18].

For the preparation of $Ce_{0.9-x}Gd_{0.1}Cu_xO_{2-\delta}$ ($0 \le x \le 0.01$), aqueous solutions of cerium nitrate and citric acid were mixed at a molar ratio of 1:3 (metal:citric acid) under stirring for 1 h at 70 °C. Stoichiometric amounts of the other nitrates solutions were added into the solution with an interval of 1 h. The temperature was slowly increased to 80 °C and ethylene glycol was added at a weight ratio of 60:40 (citric acid:ethylene glycol). The solutions were vigorously stirred by a magnetic mixer until a uniform polymeric resins containing Ce^{4+}, Gd^{3+} and Cu^{2+} cations were formed. The resulting resins were calcined at 300 °C for 2 h at a heating rate of 1 °C/min to produce the precursor powders. The thermal behavior of CGO and 1 mol% CuO-CGO precursor powders was investigated by thermogravimetry in a differential thermal analyzer (Shimadzu, DTG-60H), in the 25–800 °C temperature range, with a heating rate of 10 °C/min under air flow (50 mL/min). According to thermal analysis results, the precursor powders were calcined at 600 °C for 1 h to remove remnant carbon and to obtain crystalline reactive powders.

Powder characterization was performed by X-ray diffraction (XRD) using a Shimadzu XRD-7000 diffractometer (Cu K_α radiation, with 40 kV and 40 mA). The diffraction patterns were obtained in the angular range of $20 \le 2\theta \le 80^\circ$ in step-scanning mode (0.02°/step, 2 s/step). The lattice parameters and crystallite sizes were estimated by Rietveld refinement of the XRD data using the Maud (Materials Analysis Using Diffraction) computer program [19] and the ICDD file 75-0161. Theoretical density (d_{th}) values of CGO and 1 mol % CuO-CGO powders were calculated from the lattice parameters and copper content, according to Eqs. (1) and (2):

$$d_{th,\,CGO} = \left(4/N_A a^3\right)\left((1-x)M_{Ce} + xM_{Gd} + \left(2-x/2\right)M_o\right) \quad (1)$$

$$d_{th,CuO-CGO} = \left(4/N_A a^3\right)\left((1-(x-y))M_{Ce} + xM_{Gd} + yM_{Cu} + (2-x/2)M_o\right) \quad (2)$$

where "x" is the gadolinium content (x=0.1), "y" is the copper content ($0 \le x \le 0.01$), "a" is the lattice parameter determined by Rietveld refinement of the XRD data, "N_A" is the Avogadro number (6.022×10^{23}), and "M" is the atomic weight. Since an easy detection of changes in the lattice parameter might be extremely difficult for low dopant levels, the theoretical densities of compositions with less than 1 mol% CuO were assumed to be the same as that of synthesized CGO powder (7.224 g/cm^3). The estimation of lattice parameters for lightly CuO doped CGO would nevertheless be possible but with limited accuracy. The solubility of Cu^{2+} into ceria crystal lattice was analyzed by micro-Raman spectroscopy. The micro-Raman measurements were performed at room temperature using the 514.5 nm line of an argon ion laser as the excitation source. The powder was kept at 10 mW and a 100 μm lens was used. The powders were uniaxially pressed at 130 MPa into cylindrical pellets of 8 mm diameter and ~1.5 mm thickness and then sintered in air between 1000 and 1100 °C for 5 h (CuO-CGO compositions) and 1500 °C for 3 h (CGO). The dilatometric behavior of the 1 mol% CuO-CGO green compact was assessed to a constant heating rate of 5 °C/min using a horizontal dilatometer (DIL 402C, Netzsch, Germany). The relative density of sintered pellets was calculated from the ratio of the final density obtained by the Archimedes method and the theoretical density obtained from the lattice parameter. Microstructural characterization of polished and thermally etched (25 °C below the sintering temperature) ceramic surfaces was carried out by Scanning Electron Microscopy (SEM) on a Hitachi TM 3000 microscope equipped with an EDS detector. The electrical properties of samples with and without 1 mol% CuO were examined using electrochemical impedance spectroscopy (Solartron 1260) within a frequency range between 1 Hz and 30 MHz. The impedance spectra were recorded under ambient atmosphere (200 °C up to 700 °C), after applying porous Ag-electrodes on the surface of the samples.

3. Results and discussion

The thermogravimetric (TG) curves of gadolinia doped ceria precursor powders, with and without 1 mol% CuO are shown in Fig. 1. From the TG data, it is clear that the major weight

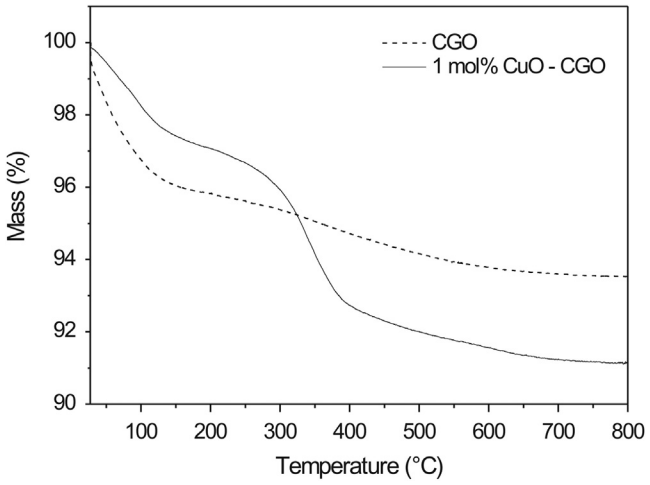

Fig. 1. Thermogravimetric curves of the precursor powders.

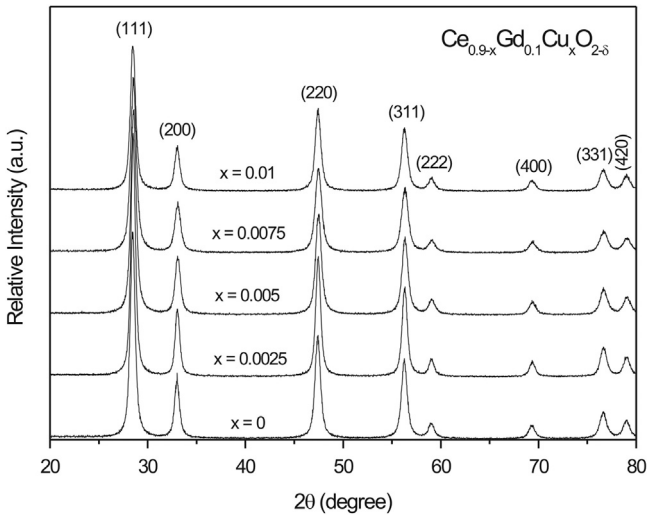

Fig. 2. XRD patterns of the $Ce_{0.9-x}Gd_{0.1}Cu_xO_{2-\delta}$ powders calcined at 600 °C.

loss occurs below 600 °C. In the temperature range between 30 and 130 °C a small weight loss (< 3%) associated with powder dehydration is observed. The next contribution to the mass loss is the burning of residual organic compounds derived from the degradation of the polymer formed by the polyesterification reaction, which is characteristic of the particular synthesis approach based on polymeric precursors. The weight loss stabilizes at approximately 700 °C. Based on these results, precursor powders were calcined at 600 °C for 1 h in view to crystallize the doped ceria phases as fine powders with high sinterability. This calcination temperature can be understood as an extremum thermal treatment condition since fine powders are likely to be obtained at lower temperatures.

The CGO composition ($Ce_{0.9}Gd_{0.1}O_{2-\delta}$) chosen for this study is justified by its high ionic conductivity in oxidizing atmospheres [1]. $Ce_{0.9-x}Gd_{0.1}Cu_xO_{2-\delta}$ ($0 \le x \le 0.01$) powders obtained by the polymeric precursor method and calcined at 600 °C for 1 h and their structural characteristics (crystal structure, lattice parameters and size crystallite) determined by powder X-ray diffraction (XRD). As observed in Fig. 2, all calcined powders are crystalline, regardless of the CuO addition. The identification of secondary phase in lightly CuO doped CGO materials is extremely difficult using X-ray diffraction since the amount of possible additional phase formed could be less than the detection limit of the XRD technique. Diffraction patterns were indexed (with no shift in their position) on the basis of CGO structure using ICDD file 75-0161, characterizing cubic fluorite type structures.

A comparative study of the crystallographic parameters was performed by Rietveld refinement using the Maud program and the results are shown in Table 1, along with the refinement parameters and calculated theoretical densities.

The lattice parameter calculated for the CGO powder ($a = 0.54185$ nm) is close to that reported in the standard ICDD card 75-0161 ($a = 0.54180$ nm) and slightly higher than that of pure ceria ($a = 0.5411$ nm, in accordance with ICDD card 34-0394). Such features indicate that there was substitution of Gd^{3+} ions in the ceria lattice, giving rise to ceria-based solid solutions.

Table 1
Comparison of crystallographic parameters of the synthesized samples with reported pattern (ICDD 75-0161).

Parameters/samples	$Ce_{0.9}Gd_{0.1}O_{2-\delta}$ (#75-0161)	$Ce_{0.9-x}Gd_{0.1}Cu_xO_{2-\delta}$	
		$x=0$	$x=0.01$
$a=b=c$ (nm)	0.54180	0.54185	0.54177
Volume (Å^3)	159.04	159.09	159.02
D_{XRD} (nm)	–	23.41	22.58
R_{wp} (%)	–	10	11.35
R_{exp} (%)	–	8.12	8.99
χ^2	–	1.23	1.26
Theoretical density (g/cm^3)	7.226	7.224	7.312

The ceria co-doping with Cu^{2+} leads to a decrease in the lattice parameter, since the ionic radius of Cu^{2+} ($r = 0.73$ Å) is smaller than that of Ce^{4+} ($r = 0.97$ Å). The crystallite sizes ($D_{XRD} = 21$–27 nm) are smaller than typical values reported in the literature, for example 40–50 nm for powders synthesized by combustion synthesis [20] and 53.7 nm for powders prepared by a complexing citrate method [21], both obtained under similar calcination conditions to the ones used in the present study. Reduced crystallite sizes typically provide higher densities of ceramics. The theoretical density calculated for 1 mol% CuO-CGO sample being higher (7.312 g/cm^3) in comparison with CGO (7.224 g/cm^3) further supports the plausible formation of the CuO-doped $Ce_{0.9}Gd_{0.1}O_{2-\delta}$ solid solution.

The solubility limit of copper into ceria crystal lattice was further analyzed by micro-Raman spectroscopy, which is more sensitive to the local structure ordering than X-ray diffraction. Fig. 3 illustrates micro-Raman spectra of $Ce_{0.9}Gd_{0.1}O_{2-\delta}$ and 1 mol% CuO-CGO powders. The Raman mode at ~460 cm^{-1} is assigned to the F_{2g} vibration of oxygen ions around Ce^{4+} ions in the CeO_8 octahedra [22]. This defect sensitive mode is shifted to lower frequencies in the case of Cu doped sample, which could be due to the increase in oxygen vacancy as a result of Cu^{2+}

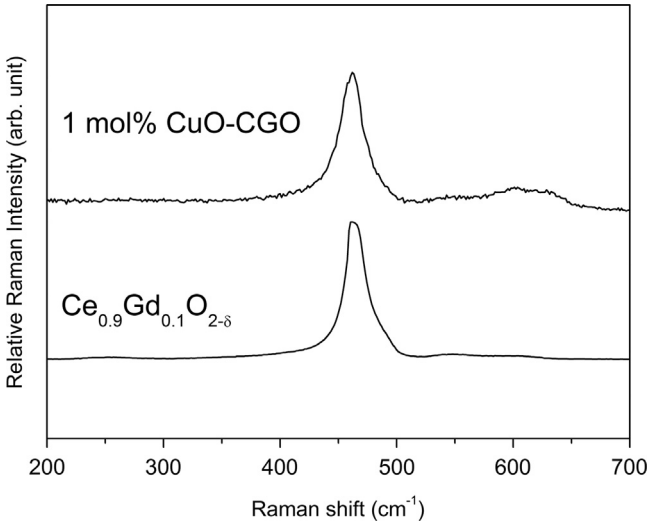

Fig. 3. Micro-Raman scattering spectra of powders calcined at 600 °C.

replacement in Ce^{4+} sites [23]. The decrease of lattice parameter with 1 mol% CuO doping as measured by XRD is complementary to the observed Raman shift as well. The lower frequency shift together with the broadening of the F_{2g} mode is an indication of disordered oxygen sublattice caused by the changed local environment due to the Cu doping. The mode at ~600 cm^{-1} is ascribed to the intrinsic oxygen vacancies in the ceria lattice [24]. The band between 550 and 650 cm^{-1} is broader for 1 mol% CuO-CGO as compared to $Ce_{0.9}Gd_{0.1}O_{2-\delta}$, which could be due to the fact that extra oxygen vacancies are created to compensate the valence mismatch between Cu^{2+} and Ce^{4+}. The characteristic Raman modes of CuO are at 288 cm^{-1} and 624 cm^{-1} [25], with the first one having higher intensity. In the present work, the peak at 288 cm^{-1} is absent and the one at 624 cm^{-1} is overlapped with the CGO peaks, which make it extremely difficult to conclude the possibility of obtaining CuO phase separately. At the outset, from the above discussions, it is reasonable to expect the formation of $Ce_{0.89}Gd_{0.1}Cu_{0.01-y}O_{2-\delta}$ solid solution with the addition of 1 mol% CuO.

Table 2 shows the results of relative density as a function of copper oxide content and sintering temperature. The CGO sample sintered at 1500 °C for 3 h has a relative density of 95%. By comparing density values in Table 2, it is evident that the co-doping with small amounts of CuO accelerates the sintering process, leading to relative densities higher than that of un-doped CGO at temperatures as low as 1000 °C.

For sintering temperature of 1000 °C, the effect of CuO addition is more pronounced for samples with $x \geq 0.5$ mol%, in which the relative density values attained 98%. The impact of 1 mol% CuO addition on sample densification was further assessed by the dilatometric analysis, shown in Fig. 4. Although previous works showed that pure CGO starts to shrink at approximately 1000 °C [12,26], 1 mol% CuO-CGO shows signs of early densification already at ~550 °C, which may be associated to the beginning of the mass transport processes. The shrinkage observed in the 600–950 °C temperature range is related to solid state diffusion, i.e., grain

Table 2
Relative density as a function of sintering temperature and CuO content.

Sintering temperature (°C)	Relative density (%)			
	Cu-free	0.25 mol% CuO	0.50 mol% CuO	1 mol% CuO
1000	–	88	98	98
1050	–	98	98	98
1100	–	95	90	93
1500	95	–	–	–

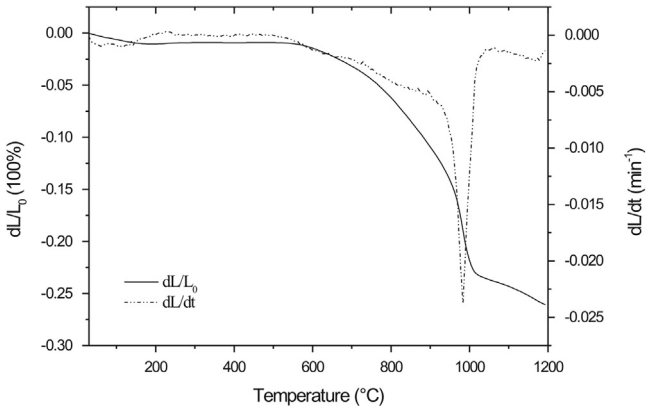

Fig. 4. Dilatometric curves for the 1 mol% CuO-CGO green sample.

boundary, surface and volume diffusion. The rapid densification at 950–1050 °C suggests a liquid phase assisted mechanism which can be ascribed to the formation of a Gd_2O_3–CeO_2–CuO ternary phase. However, the most important result is that the temperature of maximum shrinkage rate (around 1000 °C) is much lower than the often reported for pure CGO (above 1400 °C) [12]. This means that the addition of 1 mol% CuO could decrease the sintering temperature needed to attain optimum densification of $Ce_{0.9}Gd_{0.1}O_{2-\delta}$ by about 500 °C. The driving force for the densification of CuO doped CGO samples could be the presence of the small amount of liquid phase and the in turn decrease in the liquid–vapor interface area which is different from the solid state diffusion mechanism that happens in the sintering process of un-doped CGO samples.

Sintering at 1050 °C yields samples with 98% densification, regardless of the CuO content. Due to its dissolution and precipitation from the melt, the liquid phase accelerates the mass transport phenomena, resulting in rapid densification during the sintering process [16]. On the other hand, as sintering temperature is increased from 1050 to 1100 °C, there is a slight decrease in relative density, which assumes values ranging from 90% to 95%. Such a reduction of density with sintering temperature (between 1050 and 1100 °C) may be attributed to the retard of inter-granular pore elimination process during viscous flow sintering induced by the high temperature volatilization of the ternary liquid phase [12].

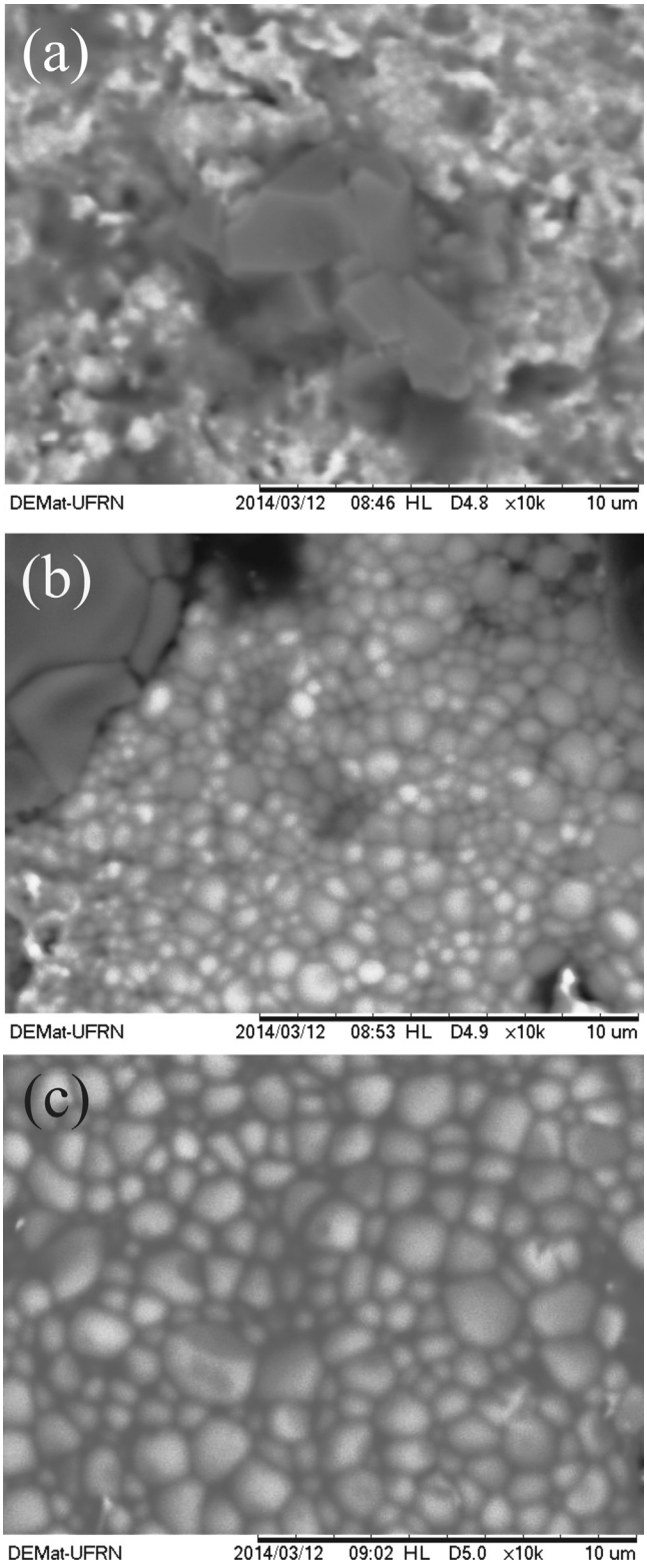

Fig. 5. Surface micrographs of 1 mol% CuO-CGO samples sintered at (a) 1000, (b) 1050 and (c) 1100 °C.

Surface micrographs of 1 mol% CuO-CGO samples (Fig. 5) sintered between 1000 and 1100 °C show that the ceramic microstructure is extremely sensitive to the sintering temperature. The sample sintered at 1000 °C (Fig. 5a) shows a dense microstructure in good agreement with the highest relative density. The images acquired using backscattered electrons allowed the identification of two micro-constituents with different sizes and morphologies. Small grains (100–300 nm, within equipment limitations) with spherical morphology are attributed to the CuO-doped CGO solid solution. Micrometric grains with poorly defined geometry are related to mixed oxide (Cu-rich) phases, which will be further proved by the energy dispersive X-ray (EDS) analyses. A similar result was found for a samaria doped ceria (SDC) sample doped with 1 mol% CuO and sintered at 1000 °C for 5 h [27]. The sample sintered at 1050 °C (Fig. 5b) also shows a dense microstructure, together with a remarkable grain growth, which is consistent with the calculated relative density. As can be observed from Fig. 5b, after sintering at 1050 °C the grain size leaves the submicron scale to values slightly above 1 μm. From 1050 to 1100 °C, a continuous grain growth of the ceria based solid solution is observed (Fig. 5c). As the sintering temperature increases the diffusion processes are favored by accelerating the mass transfer and consequently promoting the grain growth.

SEM-EDS results for the 1 mol% CuO-CGO sample sintered at 1000 °C are shown in Fig. 6. The chemical mapping of the Cu element (Fig. 6b) confirms its accumulation in the micrometer grains observed in Fig. 5a. Ce and Gd elements are homogeneously distributed in the sample (Fig. 6c–d), suggesting that besides the formation of the $Ce_{0.89}Gd_{0.1}Cu_{0.01-y}O_{2-\delta}$ solid solution (in Ce–Gd-rich regions), it is also reasonable to expect that a small amount of Ce and Gd is dissolved in the copper oxide agglomerated phase. Thus, the micrometer grains in Figs. 5 and 6a can be attributed to mixed oxides (Cu-rich) based on Cu, Ce and Gd elements.

A comparative study between the fracture surfaces of 1 mol% CuO-CGO samples sintered at 1050 and 1100 °C is shown in Fig. 7. As can be seen, the sample sintered at 1050 °C (Fig. 7a) is much denser than the one sintered at 1100 °C (Fig. 7b). The closed pores observed in both samples are characteristic of the viscous flow sintering taking place as a result of the liquid phase formation at high temperatures (promoted by 1 mol% CuO). Besides, the increase in pore content with increasing the sintering temperature from 1050 to 1100 °C was closely related to the fact that CuO is much more evaporable compared to other sintering aids, such as Fe_2O_3, CoO and NiO [28].

Electrochemical impedance spectroscopy was used to study the electrical properties of Cu-free and 1 mol% CuO doped CGO samples sintered at 1500 and 1000 °C, respectively. Fig. 8 shows a typical impedance spectrum (normalized using the geometric factor) for 1 mol% CuO-CGO sample measured at 230 °C in air. The spectrum consists of high, intermediate, and low frequency parts which may be ascribed to the contributions from grain (R_g), grain boundary (R_{gb}), and electrode resistance, respectively. The sample shows higher grain boundary impedance in comparison with the bulk impedance which is reasonable for the doped ceria samples. The distinct sets of total conductivity (σ) values, the significant ones considering SOFC applications, were calculated from the total ohmic resistance ($R_g + R_{gb}$) derived from the impedance

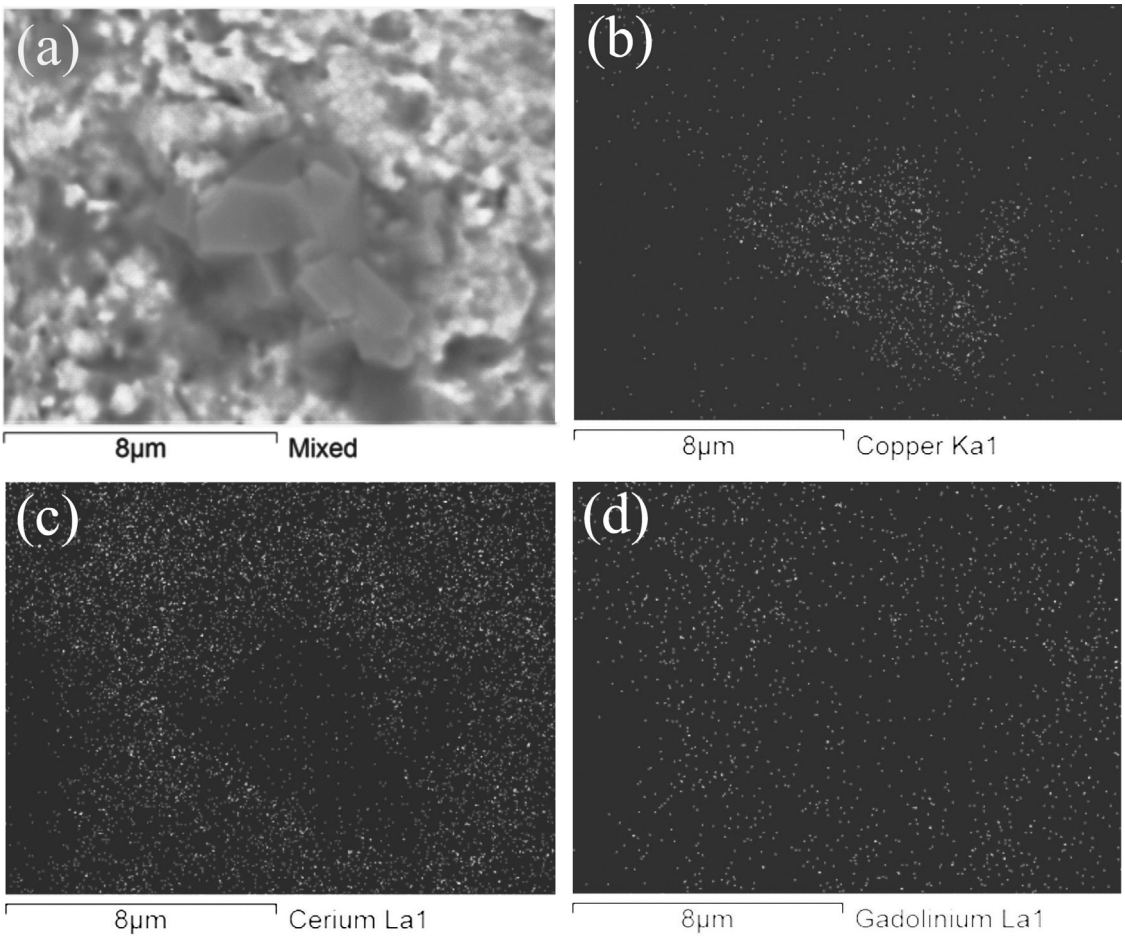

Fig. 6. Surface SEM-EDS analyses of the 1 mol% CuO-CGO sample sintered at 1000 °C: (a) micrograph, (b) Cu element mapping, (c) Ce element mapping, and (d) Gd element mapping.

spectra (corresponding to the intercept of the grain boundary arc with the real axis). These sets of conductivity values were further plotted against the temperature using a classical Arrhenius-type law to extract the corresponding activation energies.

Arrhenius-type plots of total conductivity are presented in Fig. 9. In the low temperature region (≤ 500 °C), a clear decrease in conductivity was observed for the CuO containing sample. A deeper analysis of the Arrhenius type behavior is difficult due to the limited data points available from the impedance measurements. The electrical behavior of the CuO-free sample was similar to that usually observed for polycrystalline doped ceria oxides [29,30]. At elevated temperatures, the electrical conduction is controlled by the population of charge-carrying defects (oxygen vacancies), which is expected to be higher for the co-doped sample. The conductivity of our $Ce_{0.89}Gd_{0.1}Cu_{0.01-y}O_{2-\delta}$ electrolyte measured at 600 °C ($\sigma = 15.5 \times 10^{-3}$ S cm^{-1}) is slightly higher than that (12.5×10^{-3} S cm^{-1}) Cu-free CGO sample and the trend is at par with that reported by Dong et al. and Boas et al. [31,32]. It demonstrates that CuO is a good sintering aid without detrimental effects on the conductivity of CGO at target working temperatures for SOFC applications.

4. Conclusions

CuO-doped $Ce_{0.9}Gd_{0.1}O_{2-\delta}$ (CGO) ceramics were synthesized by the polymeric precursor method at low temperature. The crystallographic studies confirmed the formation of ceria based solid solutions after adding both Gd^{3+} and Cu^{2+} ions in the ceria lattice. Laser Raman analysis adds evidence for the formation of $Ce_{0.89}Gd_{0.1}Cu_{0.01-y}O_{2-\delta}$ solid solution with 1 mol% CuO addition into the fluorite structure of ceria. The strongest effect of CuO as a sintering aid was observed on the relative density, mainly at temperatures around 1000 °C and CuO contents between 0.5 and 1 mol%. For these compositional and processing conditions, the sintering of CuO containing samples is dominated by the liquid phase assisted mechanism. On the other hand, as temperature is increased from 1050 to 1100 °C, there is a slight reduction in relative density, which can be attributed to the high temperature volatilization of the liquid phase. Microstructural characterization indicates that the grain size is strongly influenced by the sintering temperature, which favors diffusion processes. The addition of 1 mol% CuO on gadolinia doped ceria showed no detrimental effect on the total electrical conductivity, which reaches 15.5 mS cm^{-1} at 600 °C in air. From these results a general conclusion is that the

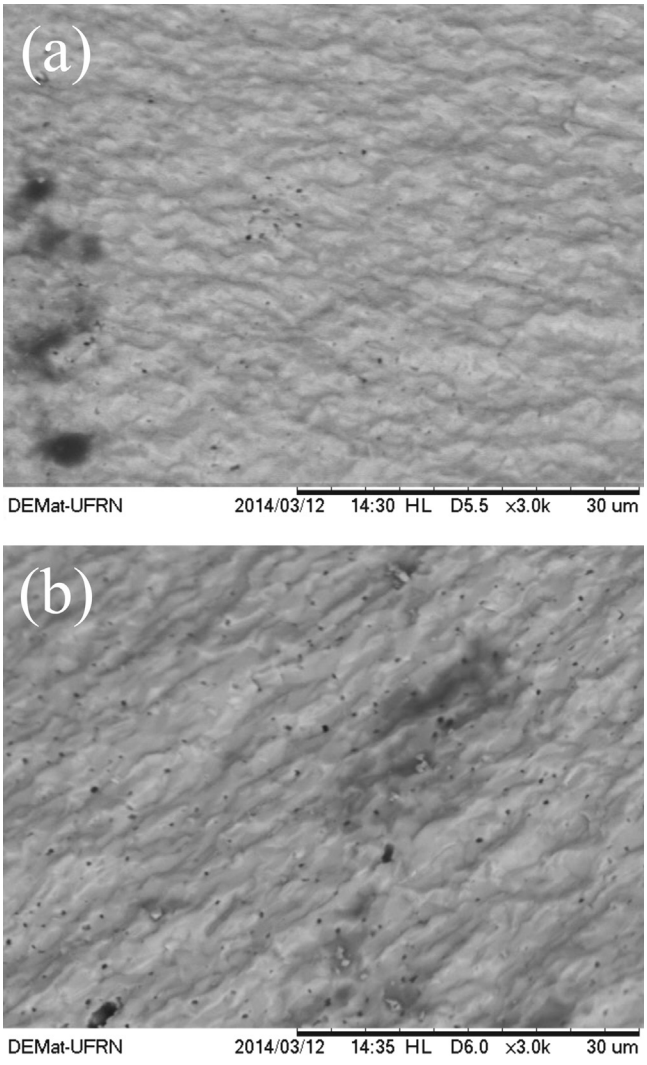

Fig. 7. Fracture surfaces of 1 mol% CuO-CGO samples sintered at (a) 1050 and (b) 1000 °C.

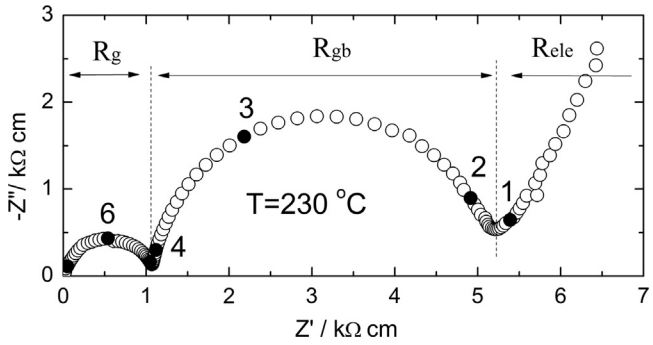

Fig. 8. Impedance spectrum of the 1 mol% CuO-CGO sample measured at 230 °C in air. The numbers close to the filled symbols are the $\log_{10}$ of the corresponding frequency.

polymeric precursor method is a viable synthesis technique to prepare $Ce_{0.89}Gd_{0.1}Cu_{0.01-y}O_{2-\delta}$ materials with potential applications as IT-SOFC electrolytes.

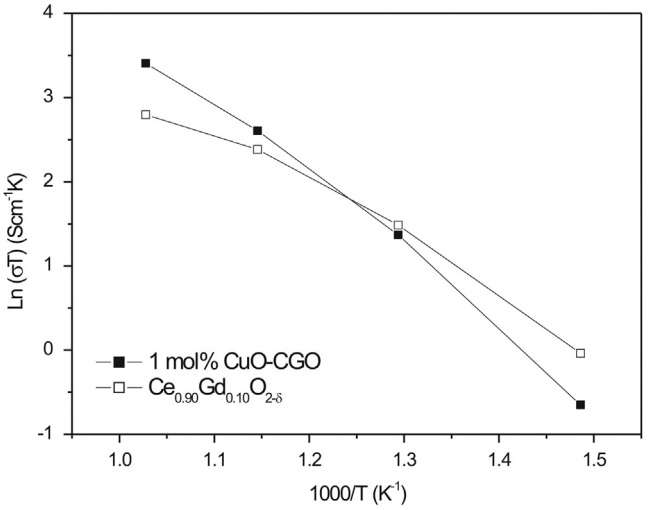

Fig. 9. Arrhenius type plots of total conductivity for $Ce_{0.90}Gd_{0.10}O_{2-\delta}$ and 1 mol% CuO-CGO samples sintered at 1500 and 1000 °C, respectively.

Acknowledgments

The authors acknowledge CAPES and CNPq (420543/2013-9) for the financial support.

References

[1] B.C.H. Steele, Appraisal of $Ce_{1-y}Gd_yO_{2-y/2}$ electrolytes for IT-SOFC operation at 500 °C, Solid State Ion. 129 (2000) 95–110.
[2] H. Inaba, H. Tagawa, Ceria-based solid electrolytes, Solid State Ion. 83 (1996) 1–16.
[3] J.A. Kilner, Fast oxygen transport in acceptor doped oxides, Solid State Ion. 129 (2000) 13–23.
[4] M. Mogensen, D. Lybye, N. Bonanos, P.V. Hendriksen, F.W. Poulsen, Factor controlling the oxide ion conductivity of fluorite and perovskite structured oxides, Solid State Ion. 174 (2004) 279–286.
[5] R.D. Shannon, Revised effective ionic radii and systematic studies of interatomic distances in halides and chalcogenides, Acta Crystallogr. A 32 (1976) 751–767.
[6] C. Fu, S.H. Chan, Q. Liu, X. Ge, G. Pasciak, Effects of transition metal oxides on the densification of thin-film GDC electrolyte and on the performance of intermediate-temperature SOFC, Int. J. Hydrog. Energy 35 (2010) 11200–11207.
[7] M. Morales, J.J. Roa, X.G. Capdevila, M. Segarra, S. Piñol, Mechanical properties at nanometer scale of GDC and YSZ used as electrolytes for solid oxide fuel cells, Acta Mater. 58 (2010) 2504–2509.
[8] J.V. Herle, T. Horita, T. Kawada, N. Sakai, H. Yokokawa, M. Dokiya, Low temperature fabrication of (Y, Gd, Sm)-doped ceria electrolyte, Solid State Ion. 86–88 (1996) 1255–1258.
[9] W. Huang, P. Shuk, M. Greenblatt, Properties of sol–gel prepared $Ce_{1-x}Sm_xO_{2-x/2}$ solid electrolytes, Solid State Ion. 100 (1997) 23–27.
[10] L.D. Jadhav, M.G. Chourashiya, A.P. Jamale, A.U. Chavan, S.P. Patil, Synthesis and characterization of nano-crystalline $Ce_{1-x}Gd_xO_{2-x/2}$ ($x=0-0.30$) solid solutionns, J. Alloy. Compd 506 (2010) 739–744.
[11] B. Cela, D.A. de Macedo, G.L. de Souza, A.E. Martinelli, R.M. do Nascimento, C.A. Paskocimas, NiO-CGO in situ nanocomposite attainment: one step synthesis, J. Power Sources 196 (2011) 2539–2544.
[12] Y. Dong, S. Hampshire, J. Zhou, G. Meng, Synthesis and sintering of Gd-doped CeO_2 electrolytes with and without 1 at% CuO dopping for solid oxide fuel cell applications, Int. J. Hydrog. Energy 36 (2011) 5054–5066.

[13] V. Gil, J. Tartaj, C. Moure, P. Duran, Rapid densification by using Bi_2O_3 as an aid for sintering of gadolinia-doped ceria ceramics, Ceram. Int. 33 (2007) 471–475.
[14] D.P. Fagg, J.C.C. Abrantes, D.P. Coll, P. Nunez, V.V. Kharton, J.R. Frade, The effect of cobalt oxide sintering aid on electronic transport in $Ce_{0.80}Gd_{0.20}O_{2-\delta}$ electrolyte, Electrochim. Acta 48 (2003) 1023–1029.
[15] S.H. Park, H.I. Yoo, Defect-chemical role of Mn in Gd-doped CeO_2, Solid State Ion. 176 (2005) 1485–1490.
[16] Y. Dong, S. Hampshire, B. Lin, Y. Ling, X. Zhang, High sintering activity Cu–Gd Co-doped CeO_2 electrolyte for solid oxide fuel cell, J. Power Sources 195 (2010) 6510–6515.
[17] R.A. Candeia, M.I.B. Bernardi, E. Longo, I.M.G. Santos, A.G. Souza, Synthesis and characterization of spinel pigment $CaFe_2O_4$ obtained by the polymeric precursor method, Mater. Lett. 58 (2004) 569–572.
[18] D.S. Gouveia, A.G. Souza, M.A.M.A. Maurera, C.E.F. Costa, I.M.G. Santos, S. Prasad, J.B. Lima, C.A. Paskocimas, E. Longo, Thermal study of the ceramic pigments $Co_xZn_{(7-x)}Sb_2O_{12}$, J. Therm. Anal. Calorim. 67 (2002) 459–464.
[19] L. Lutterotti, MAUD – Materials Analysis Using Diffraction, 2014, ⟨http://www.ing.unitn.it/∼maud/⟩.
[20] R.V. Wandekar, M. Ali, B.N. Wani, S.R. Bharadwaj, Physicochemical studies of NiO – GDC composites, Mater. Chem. Phys. 99 (2006) 289–294.
[21] R.O. Fuentes, R.T. Baker, Structural, morphological and electrical properties of $Gd_{0.1}Ce_{0.9}O_{1.95}$ prepared by a citrate complexation method, J. Power Sources 186 (2009) 268–277.
[22] W.H. Weber, K.C. Hass, J.R. McBride, Raman study of CeO_2: second order scattering, lattice dynamics, and particle size effects, Phys. Rev. B 48 (1993) 178–185.
[23] B.Z. Matovic, D.M. Bucevac, M. Rosic, B.M. Babic, Z.D. Dohcevic-Mitrovic, M.B. Radovic, Z.V. Popovic, Synthesis and characterization of Cu-doped ceria nanopowders, Ceram. Int. 37 (2011) 3161–3165.
[24] A. Nakajima, A. Yoshihara, M. Ishigame, Defect-induced Raman spectra in doped CeO_2, Phys. Rev. B 50 (1994) 13297–13307.
[25] K.I. Chiu, F.I. Kwong, D.H.L. Ng, Enhanced oxidation of CO by using a porous biomorphic $CuO/CeO_2/Al_2O_3$ compound, Microporous Mesoporous. Mater 156 (2012) 1–6.
[26] C. Goulart, E. Djurado, Synthesis and sintering of Gd-doped CeO_2 nanopowders prepared by ultrasonic spray pyrolysis, J. Eur. Ceram. Soc. 33 (2013) 769–778.
[27] X. Zhang, C.D. Petit, S. Yick, M. Robertson, O. Kesler, R. Maric, D. Ghosh, A study on sintering aids for $Sm_{0.2}Ce_{0.8}O_{1.9}$ electrolyte, J. Power Sources 162 (2006) 480–485.
[28] T. Zhu, Y. Lin, Z. Yang, D. Su, S. Ma, M. Han, F. Chen, Evaluation of Li_2O as an efficient sintering aid for gadolinia-doped ceria electrolyte for solid oxide fuel cells, J. Power Sources 261 (2014) 255–263.
[29] M.A.F. Öksüzömer, G. Dönmez, V. Sariboğa, T. Gürkaynak Altinçekiç, Microstructure and ionic conductivity properties of gadolinia doped ceria ($Gd_xCe_{1-x}O_{2-x/2}$) electrolytes for intermediate temperature SOFCs prepared by the polyol method, Ceram. Int. 39 (2013) 7305–7315.
[30] R.K. Lenka, T. Mahata, A.K. Tyagi, P.K. Sinha, Influence of grain size on the bulk and grain boundary ion conduction behavior in gadolinia-doped ceria, Solid State Ion. 181 (2010) 262–267.
[31] Y. Dong, S. Hampshire, J. Zhou, X. Dong, B. Lin, G. Meng, Combustion synthesis and characterization of Cu–Sm co-doped CeO_2 electrolytes, J. Eur. Ceram. Soc. 31 (2011) 2365–2376.
[32] L.A.V. Boas, F.M.L. Figueiredo, D.P.F. Souza, F.M.B. Marques, Zn as sintering aid for ceria-based electrolytes, Solid State Ion. 262 (2014) 522–525.